ELSEVIER

Thin Solid Films 275 (1996) 266–269

thin solid films

Surface structure characterization by photoelectron holography

M. Zharnikov [1], M. Weinelt, P. Zebisch, H.-P. Steinrück [2]

Physik-Department E20, Technische Universität München, W-85747, Garching, Germany

Abstract

The applicability of photoelectron holography to determine the structure of clean and adsorbate-covered metal surfaces is investigated. The real space structure of various systems is reconstructed from photoelectron diffraction patterns at various kinetic energies using (1) the single wavenumber and (2) the multiple wavenumber reconstruction algorithm. It is demonstrated that adsorption sites can be unequivocally identified using the multiple wavenumber approach.

Keywords: Surface structure; Metals

Photoelectron holography is a relatively new technique in surface science that has as yet to establish itself as a standard method to investigate the structure of surfaces [1–10]. Its basic idea is that a photoelectron diffraction (PED) pattern, formed by coherent interference of photoelectron wavelets reaching the detector directly or after scattering off neighbouring atoms, can be considered as a hologram [1,2]. The three-dimensional image of the local structure around the emitter can then be numerically reconstructed from this hologram using a phased two-dimensional Fourier transform [2].

We have investigated the potential of this method by applying it to simple systems, namely clean and adsorbate-covered metal surfaces. For this purpose PED patterns have been collected at different kinetic energies for the clean Pt(110)-1×2 [9] and Ni(111) surfaces [11] as well as for the p(2×2) and (5 $\sqrt{3}$ ×2) sulphur structures on Ni(111) [11,12]. The measurements were performed at the synchrotron facility BESSY in Berlin using a homebuilt angle-multichannel analyzer [13]. The PED patterns were measured in an azimuthal sector of 126°; full-hemispherical holograms were then obtained by applying symmetry operations. The holographic information was isolated from the background using the Fourier filtering technique [10]. To reconstruct the real space structure, the holograms at different kinetic energies were processed (1) individually within the single wavenumber approach [2], and (2) together within the multiple wavenumber phased sum method [3]. The main idea of the multiple wavenumber method is the summation of properly phased reconstructed amplitudes for different wavenumbers, i.e. kinetic energies. This leads to a reduction of multiple scattering and self-interference contributions as well as holographic twin images [3].

For all systems investigated, the quality of the reconstructed images (positions of atoms, intensity of artifacts) obtained using the single wavenumber algorithm strongly depends on the kinetic energy of the photoelectrons. This is illustrated by Fig. 1 where holographic reconstructions of the

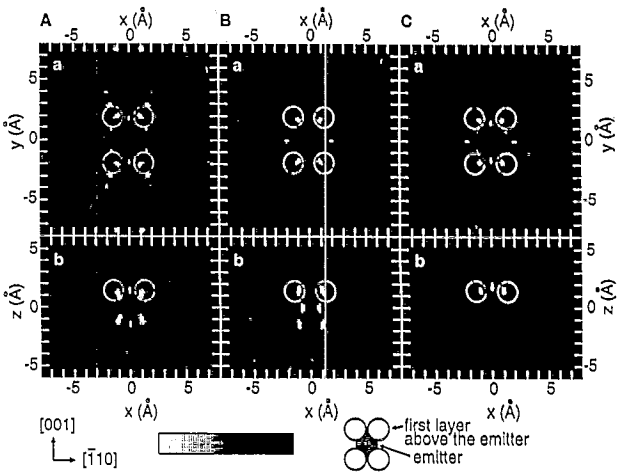

Fig. 1. Holographic reconstructions of clean Pt(110)-1x2 obtained from Pt $4f_{7/2}$ photoelectron diffraction patterns using the single wavenumber algorithm for E_{kin} = 222.4 eV (A) and E_{kin} = 369.3 eV (B), and the multiple wavenumber algorithm (C) using data at six different energies. (a) represent cuts in a plane parallel to the surface at z = 1.4 Å (the first plane above the emitter) and (b) cuts in a vertical plane parallel to the (001) plane at y = 1.96 Å. The centers of the circles mark the correct positions of the Pt atoms.

[1] Present address: MPI für Mikrostrukturphysik, Weinberg 2, D-06120 Halle, Germany.

[2] New address: Experimentelle Physik II, Universität Würzburg, D-97074 Würzburg, Germany.

SSDI 0040-6090(95)07059-1

Pt(110)-1×2 surface obtained from Pt $4f_{7/2}$ holograms at 222.4 eV (A) and 369.3 eV (B) using the single wavenumber algorithm, as well as that obtained from six Pt $4f_{7/2}$ holograms at different kinetic energies (between 120 and 370 eV) together using the multiple wavenumber method (C), are depicted: in each case (a) represents a cut in the plane parallel to the surface at $z = 1.4$ Å (the first plane above the emitter) and (b) shows a cut in a vertical plane parallel to the (001) plane at $y = 1.96$ Å. For 369.3 eV (Fig. 1(B)) the images are dominated by maxima attributed to the nearest neighbours in the plane above the emitter (the centres of the circles mark the correct positions of these atoms); for 222.4 eV (Fig. 1(A)) numerous intense artifacts are observed. The multiple wavenumber approach (Fig. 1(C)) leads to a strong suppression of the twin image, a reduction of certain artifacts and some improvement of resolution [9]. In all cases the atomic images are shifted from their true values by 0.2–0.3 Å.

For Ni(111) PED patterns of Ni $3p_{3/2}$ photoelectrons have been measured at seven different kinetic energies, ranging from 239 to 417 eV [10]. For this system, the outcome of the real space reconstructions is, however, qualitatively different from that for Pt(110)-1×2: the reconstruction in the first plane above the emitter is now dominated by intense artifacts; on the other hand, atoms in the second and third plane above the emitter and neighbouring atoms in the plane of emitter can be identified (Fig. 2). Again, the quality of the single-energy reconstructions strongly depends on kinetic energy. As a consequence, the (averaging) multiple wavenumber reconstruction in the emitter plane (Fig. 2(A-b)) as well as in the other planes contains more artifacts than the "best" single energy reconstruction at 268.8 eV (Fig. 2(A-a)). The artificial structure in the multiple wavenumber reconstruction is strongly reduced when using diffraction data within the sector of measurements only (Fig. 2(B)); this sector is indicated in the schematic drawing at the bottom of Fig. 2. Only Ni atoms inside the sector are reproduced because, due to the strong forward-scattering character of the scattering factor, only these atoms have intense diffraction fringes in that direction. For the single wavenumber reconstruction in Fig. 2(B-a), the atomic images are accompanied by the corresponding twin images that are absent in Fig. 2(B-b), as is expected for the multiple wavenumber reconstruction.

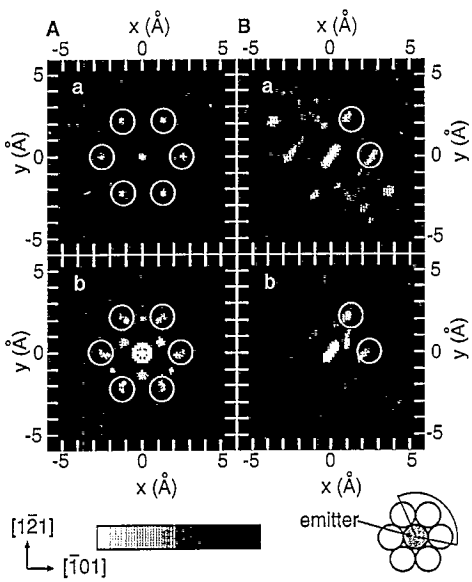

Fig. 2. Holographic reconstructions of clean Ni(111) in the emitter plane parallel to the surface ($z = 0$), obtained from the Ni $3p_{3/2}$ hologram at $E_{kin} = 268.8$ eV using the single wavenumber algorithm (a), and from seven Ni $3p_{3/2}$ holograms at different energies using the multiple wavenumber algorithm (b). (A) has been obtained from the full hologram and (B) using only diffraction data within the sector of measurements (126°, indicated in the schematic drawing at the bottom). The centers of the circles mark the correct positions of the Ni atoms (for (B) only within the sector of the measurement).

The apparent difference in the reconstruction of different atoms (relative to the source atom) for Pt(110)-1×2 and Ni(111) is attributed to the different angular-momentum character of the corresponding reference waves and to the anisotropy of the atomic scattering factor. The multiple wavenumber-phased sum method does not contain any correction for this anisotropy, which is particularly strong in the forward-scattering geometry (where the scatterers are placed between emitter and detector), that is used for the investigation of single-crystal surfaces. As a consequence, the particular nature of the scattering factor will have a strong influence on the quality of the holographic reconstruction of particular groups of atoms; this makes the achievement of reliable results rather questionable.

The anisotropy of the scattering factor is, however, much less pronounced for the backscattering geometry where the emitter is located between the scatterers and detector. This geometry is realized for very thin (up to one monolayer) metallic films or for adsorbate structures on a surface, if the PED pattern is obtained using an adlayer photoemission peak. We have measured PED patterns of S $2p_{3/2}$ photoelectrons for the p(2×2)S and $(5\sqrt{3}\times2)S$ structures on Ni(111) at seven different kinetic energies between 130 and 322.5 eV; these two sulphur superstructures have been selected due to their different complexity.

As for the clean Pt(110)-1×2 and Ni(111) surfaces, the quality of the images obtained within the single wavenumber reconstruction approach strongly depends on the kinetic energy of photoelectrons; consequently, a reliable determination of the adsorption site is not possible using one single energy only. However, the application of the multiple wavenumber-phased sum method allows the unequivocal determination of the fcc adsorption site for Ni(111)-p(2×2)S in complete agreement with results of previous investigations [14,15], as is illustrated in Fig. 3(A). In this figure the atomic images of three nearest Ni neighbours in the plane ~1.6 Å below the emitter are clearly visible from cuts in two mutually perpendicular planes: (a) corresponds to a plane parallel to the surface, 1.6 Å below the emitter and (b) represents a plane perpendicular to the surface along the [$\bar{1}$01] direction, passing through one of the atomic images. The adsorbate–substrate distance can also be determined from cut

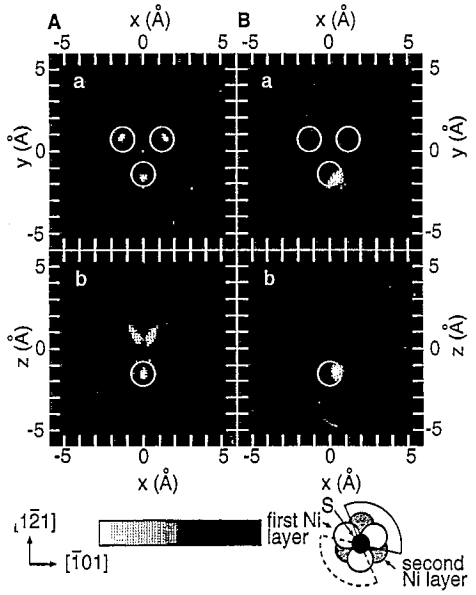

Fig. 3. Holographic reconstructions for Ni(111)-p(2×2)S from seven S $2p_{3/2}$ holograms at different energies using the multiple wavenumber algorithm: (a) represent cuts in a plane parallel to the surface at $z=-1.6$ Å and (b) cuts in a vertical plane parallel to the (1$\bar{2}$1) plane at $y=-1.59$ Å. The y value in (b) has been shifted from the correct value of $y=-1.44$ Å to pass through the atom images. (A) has been obtained from the full hologram and (B) from the experimental sector only (the experimental sector of 126° is indicated in the schematic drawing at the bottom by solid lines; the backscattering sector is indicated by dashed lines). The centers of the circles mark the correct positions of the Ni atoms for the fcc adsorption site of S on Ni(111).

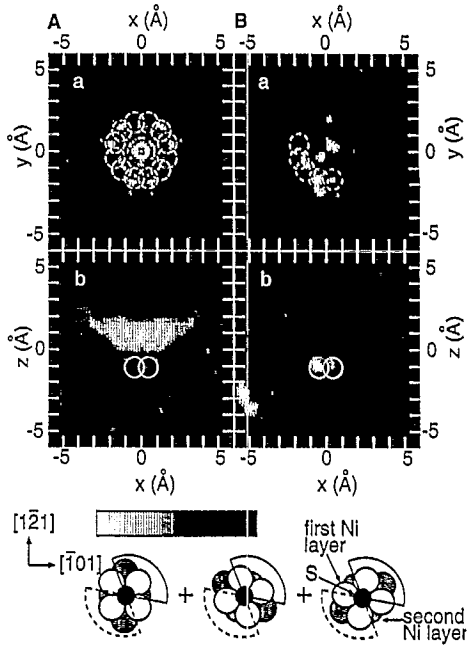

Fig. 4. Holographic reconstructions for Ni(111)-(5$\sqrt{3}$×2)S from seven S $2p_{3/2}$ holograms at different energies using the multiple wavenumber algorithm: (a) represent cuts in a plane parallel to the Ni(111) surface at $z=-1.2$ Å and (b) cuts in a vertical plane parallel to the (1$\bar{2}$1) plane at $y=-1.75$ Å. (A) has been obtained from the full hologram and (B) from the experimental sector only (the experimental sector of 126° is indicated in the schematic drawing at the bottom by solid lines; the backscattering sector is indicated by dashed lines). The centers of the circles mark the correct positions of the Ni atoms according to the structure suggested in Ref. [20].

(b) as ~1.6 Å. The atomic images of three Ni atoms completely dominate in the physically meaningful region ($z<0$) of the reconstruction. The artificial structure in the range $z>0$ partly stems from symmetry operations used to obtain the whole hologram from the experimentally determined sector; this is concluded from the fact that this structure disappears when only the sector of measurements is used for the reconstruction (Fig. 3(B)). In this case, only the Ni atom that lies almost entirely inside the backscattering sector (indicated by dashed lines in the schematic drawing at the bottom of Fig. 3) is observed which is attributed to the maximum of the scattering factor in the backscattering direction (180°).

For the (5$\sqrt{3}$×2)S structure on Ni(111) different structural models have been proposed [16–21] implying different reconstructions of the Ni(111) surface along with different S adsorption sites on the reconstructed (or non-reconstructed) surface. The holographic reconstructions of this structure are rather different from those for the p(2×2)S structure. Intense maxima are now located in the plane 1.1–1.2 Å below the emitter (parallel to the surface). Cuts in this plane (a) along with cuts in the plane perpendicular to the surface along the [$\bar{1}$01] direction passing through some of the intense maxima (b) are depicted in Fig. 4. The quality of the reconstructions is rather low which is attributed to the complexity of the (5$\sqrt{3}$×2)S structure and the superposition of the holographic contributions from different domains. Nevertheless, some qualitative and quantitative conclusions can be derived: the data are not consistent with coexistence of many different adsorption sites; furthermore, the relatively small distance of ~1.2 Å to the top Ni layer rules out a three-fold hollow adsorption site and indicates adsorption on a more open surface than an unreconstructed Ni(111). The reconstructed image is approximately consistent with a quasi-(100) reconstruction of the Ni(111) crystal surface and four-fold adsorption site of S on this surface [16,20]. For comparison, the positions of the Ni atoms according to the model are also depicted in Fig. 4 (circles) together with schematic drawing of the adsorption geometry for three different domains [20].

In conclusion, we have demonstrated that photoelectron holography can be successfully applied to determine the adsorption site of adsorbates in the backscattering geometry. For clean metal surfaces, reliable results are difficult to obtain due to the strong anisotropy of the scattering factor for forward scattering. The very large experimental data sets usually associated with photoelectron holography (full-hemispherical PED patterns at various kinetic energies) can be reduced, if diffraction data in a defined angular sector only (at best in the symmetry-irreducible one) are used for the reconstruction; this approach also leads to a reduction of artificial structures.

The main advantage of photoelectron holography is that no preliminary assumptions about the structure of the investigated system are included in the reconstruction algorithm. The application of the multiple wavenumber-phased sum

method (using PED patterns measured at different kinetic energies) allows one to avoid the problems related to the observed energy dependence of the single-energy reconstructions. Due to the limited spatial resolution of the photoelectron holography, it is not possible to determine the positions of adsorbates with very high accuracy; an approximate determination of the local structure around the emitter can, however, be realized. The structural model can thereafter (if necessary) be refined by more accurate structural methods such as low-energy electron diffraction and scanned energy PED which compare experimental data sets to calculations for various possible structures.

Acknowledgements

This work has been supported by the DFG (SFB 338) and by the BMFT (05 5WO CAI).

References

[1] A. Szöke, in D.T. Attwood and J. Boker (eds.), *Short Wavelength Coherent Radiation: Generation and Application*, AIP Conf. Proc., No. 147, AIP, New York, 1986.
[2] J.J. Barton, *Phys. Rev. Lett., 61* (1988) 1356.
[3] J.J. Barton, *Phys. Rev. Lett., 67* (1991) 3106.
[4] D.K. Saldin, G.R. Harp and B.P. Tonner, *Phys. Rev., B45* (1992) 9629.
[5] S.Y. Tong, H. Huang and C.M. Wei, *Phys. Rev., B46* (1992) 2452.
[6] Hua Li, S.Y. Tong, D. Naumovic, A. Stuck and J. Osterwalder, *Phys. Rev., B47* (1993) 10036.
[7] L.J. Terminello, J.J. Barton and D.A. Lapiano-Smith, *Phys. Rev. Lett., 70* (1993) 599.
[8] S.Y. Tong, Hua Li and H. Huang, *Phys. Rev. Lett., 67* (1991) 3102.
[9] M. Zharnikov, D. Mehl, M. Weinelt, P. Zebisch and H.-P. Steinrück, *Surf. Sci., 312* (1994) 82.
[10] M. Zharnikov, D. Mehl, M. Weinelt, P. Zebisch and H.-P. Steinrück, *Surf. Sci., 306* (1994) 125.
[11] M. Zharnikov, M. Weinelt, P. Zebisch, M. Stichler and H.-P. Steinrück, *Surf. Sci., 334* (1995) 114.
[12] M. Zharnikov, M. Weinelt, P. Zebisch, M. Stichler and H.-P. Steinrück, *Phys. Rev. Lett., 73* (1994) 3548.
[13] H.A. Engelhardt, W. Bäck, D. Menzel and H. Liebl, *Rev. Sci. Instrum., 52* (1981) 835; H.A. Engelhardt, A. Zartner and D. Menzel, *Rev. Sci. Instrum., 52* (1981) 1161.
[14] J.E. Demuth, D.W. Jepsen and P. Marcus, *Phys. Rev. Lett., 32* (1974) 1182.
[15] Y.K. Wu and K.A.R. Mitchell, *Can. J. Chem., 67* (1989) 1975.
[16] T. Edmonds, J.J. McCarrol and R.C. Pitkethly, *J. Vac. Sci. Technol., 8* (1971) 68.
[17] W. Erley and H. Wagner, *J. Catal., 53* (1978) 287.
[18] P. Delescluse and A. Masson, *Surf. Sci., 100* (1980) 423.
[19] L. Ruan, I. Stensgaard, F. Besenbacher and E. Laegsgaard, *Phys. Rev. Lett., 71* (1993) 2963; *72* (1994) 2500.
[20] D.E. Gardin, J.D. Batteas, M.A. Van Hove and G.A. Somorjai, *Surf. Sci., 296* (1993) 25.
[21] M. Foss, R. Feidenhans'l, M. Nielsen, E. Findeisen, R.L. Johnson, T. Buslaps, I. Stensgaard and F. Besenbacher, *Phys. Rev. Lett., B50* (1994) 8950.